Journal of Biomedical Optics

SPIEDigitalLibrary.org/jbo

Spectroscopic methods for the photodiagnosis of nonmelanoma skin cancer

Eleni Drakaki
Theognosia Vergou
Clio Dessinioti
Alexander J. Stratigos
Carmen Salavastru
Christina Antoniou

SPIE

Spectroscopic methods for the photodiagnosis of nonmelanoma skin cancer

Eleni Drakaki,[a] Theognosia Vergou,[a] Clio Dessinioti,[a] Alexander J. Stratigos,[a] Carmen Salavastru,[b] and Christina Antoniou[a]
[a]University of Athens, Department of Dermatology and Photobiology, Andreas Syggros Hospital, 5, I. Dragoumi Street, 16121 Athens, Greece
[b]"Carol Davila" Medical School, Clinic of Dermatology "Colentina" Clinical Hospital, Bucharest, Romania

Abstract. The importance of dermatological noninvasive imaging techniques has increased over the last decades, aiming at diagnosing nonmelanoma skin cancer (NMSC). Technological progress has led to the development of various analytical tools, enabling the *in vivo/in vitro* examination of lesional human skin with the aim to increase diagnostic accuracy and decrease morbidity and mortality. The structure of the skin layers, their chemical composition, and the distribution of their compounds permits the noninvasive photodiagnosis of skin diseases, such as skin cancers, especially for early stages of malignant tumors. An important role in the dermatological diagnosis and disease monitoring has been shown for promising spectroscopic and imaging techniques, such as fluorescence, diffuse reflectance, Raman and near-infrared spectroscopy, optical coherence tomography, and confocal laser-scanning microscopy. We review the use of these spectroscopic techniques as noninvasive tools for the photodiagnosis of NMSC. [DOI: 10.1117/1.JBO.18.6.061221]

Keywords: fluorescence spectroscopy; diffuse reflectance spectroscopy; Raman spectroscopy; near-infrared spectroscopy; optical coherence tomography; confocal laser-scanning microscopy; nonmelanoma skin cancer; noninvasive photodiagnosis.

Paper 12647SS received Sep. 28, 2012; revised manuscript received Nov. 19, 2012; accepted for publication Nov. 19, 2012; published online Dec. 17, 2012.

1 Introduction

The skin is one of the tissues most investigated using optical spectroscopy because of its easy access and the great diversity of skin alterations that give significant changes in optical properties.[1] Cutaneous squamous cell carcinoma (SCC) and basal cell carcinoma (BCC), commonly termed 'nonmelanoma skin cancer' (NMSC) or 'epithelial skin cancers,' are among the most common cancers in white-skinned populations. While malignant melanoma originates from melanocytes, NMSC arises from keratinocytes. Despite its low mortality rate, BCC may cause considerable morbidity as it may occasionally grow aggressively causing extensive local tissue destruction or recurrences after treatment.[2] Cutaneous SCC, is associated with a 0.5% to 5% risk of metastasis in the general population, and often displays a more aggressive and difficult-to-treat course.[3]

Existing treatments, however, often do not meet the challenge of an effective management,[3] especially in patients with multiple lesions, advanced or widespread disease, highlighting the need for early diagnosis. Recent developments in optical imaging techniques may provide the possibility of real-time noninvasive, high-resolution analysis of skin and can potentially decrease morbidity and mortality in NMSC. Novel diagnostic methods, using the fluorescence and reflectance spectroscopic modes have been introduced to detect human tumors based on the spectral properties of tissue, avoiding the need for a skin biopsy. Several of these technologies have become commercially available, including light-induced fluorescence (LIF) and diffused reflectance spectroscopy (DRS), optical coherence tomography (OCT), near-infrared and Raman spectroscopy, multispectral fluorescence polarization imaging, and reflectance or fluorescence confocal microscopy.[4,5] In this review, we will address spectroscopic well-established as well as upcoming and bench techniques used for the photodiagnosis of NMSCs.

Address all correspondence to: Christina Antoniou, University of Athens, Department of Dermatology and Photobiology, Andreas Syggros Hospital, 5, I. Dragoumi Street, 16121 Athens, Greece. Tel: 210-7258476; Fax: 210-7240960; E-mail: christinaantoniougr@yahoo.com

2 Fluorescence

Light-induced fluorescence spectroscopy is a very attractive potential diagnostic technique for early diagnosis and demarcation of skin cancer due to its high sensitivity, easy-to-use methodology for real-time measurements, and noninvasiveness. Fluorescence emission from malignant skin tissue is usually excited using as an irradiation source a laser, light-emitting diode (LED), a xenon, or halogen lamp.

2.1 *Autofluorescence Spectroscopy*

Laser-induced fluorescence (LIF) has been proposed for the diagnosis of NMSC.[6–11] Autofluorescence imaging is an attractive potential tool due to lack of need for contrast agents' application on the tissue under investigation. It allows differentiation on the base of differences in biochemical content and metabolic state of the pathology.[1,12–14] After illumination of the tissue with an appropriate light source, the photons diffuse in the tissue and fluorescence is re-emitted, enabling noninvasive spectroscopic measurements and the 'optical biopsy' approach.[1]

Skin components, like aromatic aminoacids: phenylalanine, tryptophan, and tyrosine fluoresce under excitation with deep ultraviolet (UV) (in the spectral region 260 to 300 nm). Structural proteins: collagen and elastin and their cross-links fluorescent under excitation with 320 to 400 nm, in addition with nicotinamide adenine dinucleotide (NADH) and flavins, which are indicators of metabolic alterations, in the cutaneous

0091-3286/2012/$25.00 © 2012 SPIE

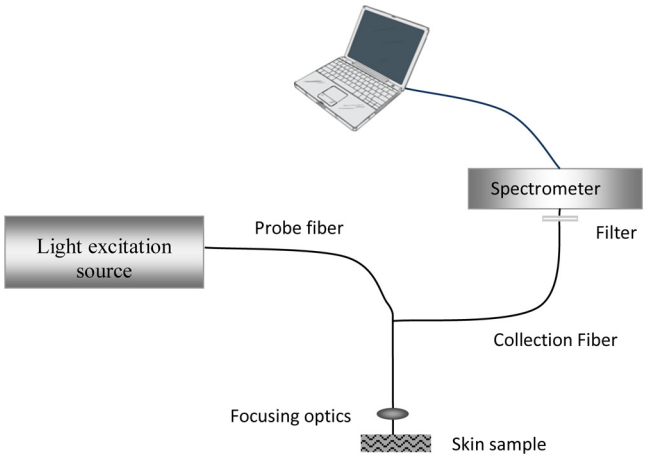

Fig. 1 Schematic diagram of the light-induced fluorescence.

tissue.[15–19] As far as the source of autofluorescence excitation of skin components is concerned, various light sources in UV and the blue-green spectral region are used for excitation of autofluorescence in skin tissues.[1,16,20–23] A scheme of a typical setup for autofluorescence spectroscopy is shown in Fig. 1.

Researchers in 2001, such as Brancaleon et al.,[20] observed higher fluorescence intensity in nonmelanoma skin tumors versus normal skin, using UV excitation for the tryptophan residues, which may be a result of epidermal thickening in the tumor site. In contrast, the fluorescence intensity associated with collagen cross-links was lower in tumors, because of the erosion and degradation of the connective tissue and the decrease in collagen and elastin crosslinks.[20]

In 2002, Panjehpour et al. studied 49 patients [BCC, SCC, actinic keratoses (AK), and normal skin] and compared diagnostic accuracy in laser-induced fluorescence spectroscopy for skin types I to III to determine the skin colors' effect on the results.[22] Normal skin exhibited stronger fluorescence emission than BCC and SCC with 410 nm excitation. The accuracy of classifying NMSC was 93% in type I skin and 78% for type III, due to the higher absorption of melanin.[5,22]

Different excitation wavelengths exhibited lower fluorescence signal in BCC tumors, in comparison with normal skin fluorescence, which is observed by the group of Na et al.,[16] Zeng et al.,[24] Borisova et al.,[25,26] and Drakaki et al.[1] In addition, a red shift of the spectral profile of BCC skin biopsies *ex vivo* was revealed during the research of optical characterization of normal and malignant skin after excitation with a nitrogen laser by Drakaki et al.[1] An example of that spectroscopic process is shown in Fig. 2.

In the wavelength spectrum of 350 to 450 nm, the higher fluorescence intensity shown in the normal tissues is due primarily to a conversion of collagen (emission around 390 to 405 nm) and elastin (emission around 400 to 410 nm) from normal to malignant tissues and a decrease in NADH (emission around 440 to 460 nm) levels in the malignant tissues.[1]

However, skin is a complex multilayered and inhomogeneous organ, with spatially varying optical properties that complicate the quantitative analysis of the fluorescence spectra.[27] In addition, the intensity of the fluorescence signal may not be a consistent parameter for a decision as several factors, such as surface morphology of the distance between the tissue surface and probe, can affect the signal. Diagnostic algorithms are able

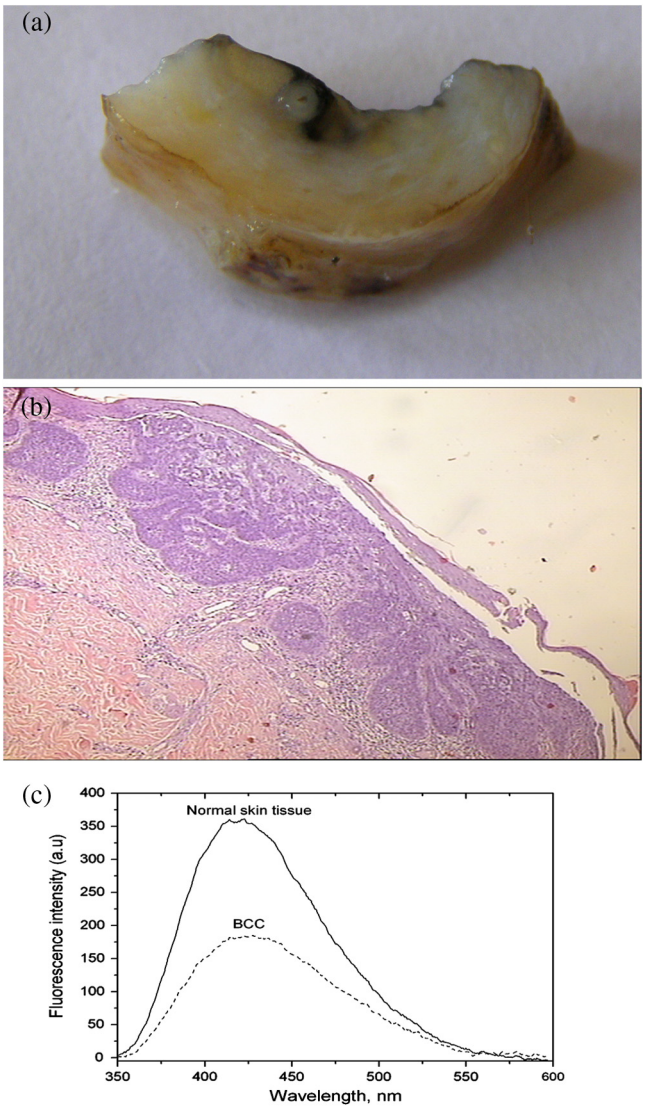

Fig. 2 (a) A representative photo of skin sample with BCC. (b) Histopathologic image in BCC area of the skin sample of part (a) (H&E). (c) Fluorescence spectra of healthy skin tissue and skin tissue with basal cell carcinoma after excitation with 337 nm of nitrogen laser.

to correlate the varied spectra and differentiate malignant tumors from normal tissues.[1,5,19,28]

2.2 *Light-Induced Fluorescence Spectroscopy with Exogenous Agents*

Exogenous fluorescent markers are used when the skin lesion is highly pigmented and the obtained fluorescence signal is too weak to be used for diagnostics.[19] In addition, special photosensitizers are introduced in the fluorescence diagnostic therapeutic modality through photodynamic therapy (PDT).

2.2.1 *PDT-associated fluorescence diagnostics: the photodynamic diagnosis*

PDT combines three elements: oxygen, light, and a photosensitizing chemical agent, such as porphyrin, to activate reactive oxygen species within targeted tissues. When this occurs, cancer cells are destroyed without damaging healthy tissue.[29] The photosensitizing agent, most commonly 5-aminolevulinic acid

(5-ALA) or methyl-aminolaevulinate (MAL) is applied either topically or systemically where it is absorbed by normal and mainly by abnormal tissue. The topical formulation generally is preferred for cutaneous disease because systemic porphyrin administration is associated with prolonged photosensitivity.[30] PDT has proven to be clinically effective in treatment of superficial skin (pre)malignancies including superficial BCC, and thin nodular BCC lesions. PDT may also prevent the development of certain NMSCs in immune-suppressed patients.[31,32] In most clinical studies 16% MAL and 20% ALA are used. At this moment, only the commercial form of MAL (Metvix®, Galderma, Paris, France) is approved in most European countries for the treatment of AKs, Bowens' disease, superficial BCC, and small nodular BCC.

The use of Protoporyphrin IX (PpIX) fluorescence for the diagnosis of NMSC is known as photodynamic diagnosis (PDD). The topical application of 5-aminolevulinic acid (5-ALA) results in a selective accumulation of Protoporyphrin IX (PpIX) in cells of NMSC. A study from Van der Beek et al.[33] compared PpIX fluorescence with and without auto-fluorescence after 5-ALA application and irradiation of pulsed light at 407 nm, for the photodiagnosis of NMSC in 30 patients. They used devices which measure not only the PpIX fluorescence, but also the auto-fluorescence of the skin.[34] The use of autofluorescence allowed for the correction of factors influencing both for autofluorescence and PpIX fluorescence equally, such as scaling, stratum corneum thickness, reflection due to a nonperpendicular alignment of the skin, or a change in the irradiance due to a variance in the distance between the skin and the light source. This way the intensity of PpIX fluorescence relative to the autofluorescence could be calculated (normalized method).[20] The specificity of the non-normalized and the normalized method of their study was 27% and 100%, respectively, while sensitivity was 39% and 97%, respectively (p-value <0.001).[33] Similar reports showed promising results in demarcation of skin lesions in 15 BCC patients.[35]

In another study, PDD has been suggested as an *in vivo* presurgical tool to determine the tumor margins before Mohs micrographic surgery.[36] The red PpIX fluorescence at 635 nm of MAL-treated BCC ($n = 35$) during illumination of blue light (365 to 405 nm) was recorded by Sandberg et al.[36] with a filtered charge-coupled device (CCD) camera, which recorded the fluorescence emission in the range of 610 to 715 nm. They had proposed MAL for higher tumor contrast compared to ALA in BCCs.[36] This superiority and its selectivity was supported by Fritsch et al.,[37] Moan et al.,[38] Kleinpenning et al.,[39] and Tierney et al.[40]

On the other hand, future research showed that preoperative fluorescence diagnosis for nodular BCC in the H-zone did not show any additional benefit compared to clinical diagnosis.[41]

Kleinpenning et al.[39] observed that there could be a potential applicability of fluorescence diagnosis with ALA-induced porphyrins to diagnose premalignant lesions with a tendency to progress into SCC and early invasive squamous skin cancer. They noticed that as SCC is characterized by hyperkeratosis and the invasion of atypical keratinocytes in the dermis with a dense inflammatory infiltrate, it is likely that the penetration of the precursor of PpIX and/or the light are the limiting factors for fluorescence diagnosis with ALA-induced porphyrins in SCC. The photosensitiser ALA was also successfully used to guide biopsy and screen for residual tumor after PDT, in a patient with SCC.[42] On the other hand, using 20% ALA to map boundaries based on the red fluorescence of the Wood's lamp in 142 patients with SCC, Bowen's disease or BCC, before Mohs micrographic surgery, did not affect the number of surgical stages necessary.[43]

Limitations of PDD include the variation of the fluorescent contrast according to the depth and thickness of the tumor, the type of photosensitizer, and the duration of application.[43]

2.2.2 *In vitro fluorescence-polarization imaging*

Yaroslavsky et al.[44] used tetracycline (TCN) and demeclocycline (DMN) fluorescence for the detection and delineation of nonmelanoma skin tumors *in vitro*. However, the success rates of TCN and DMN fluorescence emission imaging were 13% and 20%, respectively. In contrast, in the fluorescence polarization image (FPI) was successful in 88% and 94% of cases, respectively, with the cancerous area being bright, as compared to normal skin, when they were excited by linearly polarized monochromatic light centered at 390 nm. The shape, size, and location of the tumor in the FPI correlated well with histopathology. The level of endogenous fluorescence polarization was much lower than that of exogenous, and the average values of fluorescence polarization of tetracycline derivatives were significantly higher in cancerous as compared to normal tissue. The higher values of fluorescence polarization in cancer cells has been attributed to the high affinity of tetracyclines for mitochondria that are abundant in cancer cells and to changes in biochemical and optical properties of the lesional skin. It was proposed that imaging of tetracycline fluorescence polarization enables "optical sectioning" of the thick tissues, thus allowing imaging of the superficial tissue layers only. In the multiply scattering media, such as skin, fluorescence at different depths can be monitored using polarized light.[44]

3 Diffuse Reflectance Spectroscopy

The diffuse reflectance spectrum reflects the absorption and the scattering properties of the skin tissue, where the absorption coefficient is directly related to the concentration of physiologically relevant absorbers in the tissue, and the scattering coefficient reflects the size and the density of the scattering centers in tissue.[1] As the detected diffuse reflectance signal is superposition from diffuse scattering and absorption from tissues' pigments, the resultant spectrum can reveal information about main absorbers in the skin tissues, like hemoglobin and melanin and its pathologies and can provide valuable information regarding both tissue morphology and function and identify benign and cancerous or cancer prone skin lesions for the purpose of reducing unwanted benign biopsies.

A number of diffuse reflectance-based techniques have been developed for the evaluation of nonmelanoma.[45–47] The advantage of a DR spectroscopic device lies in its binary diagnosis (cancer/no cancer) making it an attractive monitoring method, that can be operated with minimal additional training.

Most of the researchers found lower spectral intensities in BCC skin tissues compared to the corresponding normal skin.[28,48] Thomson et al.[48] were able to diagnose BCCs and neighboring healthy skin, using linear discriminant analysis in a leave one-out protocol, with a sensitivity and specificity of 100% and 71% respectively. Rajaram et al.[28] found statistically significant differences ($p < 0.05$) in the optical properties between normal skin and the different histologic groups, like BCC, SCC, and AK. One explanation according to Rajaram et al.[28] is the possible breakdown in the collagen matrix present in the dermis. The contribution of collagen to the overall scattering

at the source-detector separation exceeds that of cells and nuclei. Because of this, a small increase in the epidermal scattering due to large-scale malignant cell proliferation would still be masked by a larger reduction in dermal collagen scattering. This trend in scattering from normal to malignant cancer is consistent with studies of other researchers on skin, where the scattering coefficient was significantly lower for every cancerous group, when compared to normal skin.[45,49] DRS spectra from Rajaram et al [28,50] exhibited a large flattening of the diffuse reflectance spectrum at approximately 420 nm corresponding to the Soret band of hemoglobin absorption, while change in line shape of the diffuse reflectance spectra of BCC showed large depressions in the Q-bands (540 to 575 nm) of hemoglobin absorption too. Similar trends were also noticed for AK and SCC, however, these were not found to be statistically significant. Based on statistic and mathematical analysis they determined the values of mean vessel diameter for both normal skin and BCC and they reported that the change in mean vessel diameter from normal skin (15 ± 2 μm) to BCC (40 ± 6 μm) is statistically significant.[50]

When autofluorescence is detected *in vivo*, researchers need to take into account the influence of cutaneous absorbers and scatterers, which distort the spectral shape of the autofluorescence signal coming from the tissue. To remove distortions introduced in measured tissue fluorescence spectra by tissue scattering and absorption, the fluorescence spectra may be analyzed in combination with information from the corresponding reflectance spectra. This way, the intrinsic tissue fluorescence may be extracted.[7] In addition, application of DRS could be combined with fluorescence also in highly pigmented, which exhibit too fluorescence signal.[1,19] Therefore, in the recent years, there has been growing interest in the common use of light-induced autofluorescence and reflectance spectroscopy to differentiate disease from normal surrounding tissue, mainly for detection and differentiation of cancerous and precancerous changes in human body.

Unfortunately there has been variability between and within the DR spectra groups and a classification difficulty due to the heterogeneity of lesions and anatomic differences, inter-patient differences in factors such as skin photo-type, level of sun exposure and age. There is a need for localization of the measurement volume and support for development of improved classifiers on groups of lesions, divided by specific lesion pathology.[48]

4 Raman Spectroscopy

Raman spectroscopy has strong potential for providing noninvasive dermatological diagnosis of NMSC. Raman scatters in tissues, including the cell cytoplasm, cell nucleus, fat, collagen, cholesterol-like lipid deposits, and water.[15]

Fendel et al.,[51] Gniadecka et al.,[52] Nunes et al.,[53] Schrader et al.,[54] Skrebova et al.,[55] and Barry et al.,[56] used Fourier transform (FT)–Raman spectroscopy to distinguish between BCC and surrounding normal tissue.

Gniadecka et al.[57] indicated alterations in protein and lipid structure in NMSC. Spectral changes were observed in protein bands, amide I (1640 to 1680 cm^{-1}), amide III (1220 to 1300 cm^{-1}), and n(CC) stretching (probably in amino acids proline and valine, 928 to 940 cm^{-1}), and in bands characteristic of lipids, CH2 scissoring vibration (1420 to 1450 cm^{-1}), and -(CH2)n- in-phase twist vibration around 1300 cm^{-1}.

Nijssen et al.[58] demonstrated pseudo-color Raman maps based on FT–Raman spectra obtained from a frozen tissue section of BCC. In their work, they showed that the pseudo-color Raman map is closely related to the microscopic image of the hematoxylin and eosin (H&E)-stained sample.

Silveira et al.[59] used a near-infrared Raman spectrometer to obtain spectra of normal skin and BCC *in vivo*. There were notable differences in the Raman peak intensities at 800 to 1000 cm^{-1}, 1200 to 1400 cm^{-1}, and around 1600 cm^{-1}. The authors implemented a diagnostic model to discriminate BCC from normal skin, using algorithms such as principal components analysis (PCA) and Mahalanobis distance. They reported 85% accuracy in differentiating normal skin from BCC.

R. de M. F. Pereira et al[60] used the FT-Raman spectroscopy to differentiate between normal skin and SCC *in vitro*, where spectra in the normal tissue showed the presence of vibrational bands in 860 and 939 cm^{-1} with higher intensity than in the carcinoma spectra. These modes were assigned to the vibration of proline and hydroxiproline. The shift region of 1555 to 1560 cm^{-1} showed a difference of intensity to the samples of SCC, which were attributed to the nucleic acid.

Several studies with FT–Raman spectroscopy has applied a long wavelength excitation laser (1064 nm Nd:YAG laser or 850-nm titanium–sapphire laser) in order to minimize autofluorescence from skin tissue. However, the longer wavelength laser had poor Raman scattering intensities compared to the shorter excitation wavelength laser. As a result, previously reported Raman spectra on BCC tissues show poor signal-to-noise ratios and require statistical adjustment of spectroscopic data, such as PCA,[53] K-mean clustering analysis (KCA),[58] and neural networks[52] to differentiate between Raman signals of cancerous and normal tissues.

Choi et al.[61] showed that with confocal Raman microscopy, using a shorter wavelength argon ion laser at 514.5 nm, distinct Raman band differences up to 95% between normal and BCC tissues for the amide I mode and the PO_2^- symmetric stretching mode were found, without the need for statistical adjustment of spectral data. It was also possible to precisely differentiate BCC tissue from surrounding noncancerous tissue using the confocal Raman depth profiling technique.

However, none of these groups have explored the ability of Raman spectroscopy to provide diagnosis of NMSC (BCC and SCC) and inflamed scar tissue *in vivo* at scarred areas of previous biopsy or surgical resection, particularly important for the dermatologist. Lieber et al.[62] predicted correctly with a diagnostic algorithm all of the BCC, SCC, and inflamed scar tissues and normal tissues with a 100% sensitivity, 91% specificity for abnormality, and with a 95% overall classification accuracy.

5 Near-Infrared Spectroscopy

Infrared spectroscopy and Raman spectroscopy are two mutually complementary methods, which provide information on molecular composition and structure and interactions occurring in the sample.[63]

In 1999, McIntosh et al. showed that biopsies from BCC, SCC, and melanocytic tumors have distinct mid-IR signatures compared to normal skin.[64,65] McIntosh et al.[64] used infrared spectroscopy to examine BCC to explore distinctive characteristics versus normal skin samples and other skin neoplasms. Spectra of epidermis, tumor, follicle sheath, and dermis were acquired from unstained frozen sections, and analyzed qualitatively, by t-tests and by linear discriminant analyses. Dermal spectra were significantly different from the other skin components mainly due to absorptions from collagen in dermis. Spectra of normal epidermis and BCC were significantly different by

virtue of subtle differences in protein structure and nucleic acid content. Linear discriminant analysis characterized spectra as arising from BCC, epidermis, or follicle sheath with 98.7% accuracy. Use of linear discriminant analysis accurately classified spectra as arising from epidermis overlying BCC versus epidermis overlying nontumor-bearing skin in 98.0% of cases. Spectra of BCC, SCC, nevi, and malignant melanoma were qualitatively similar. Distinction of BCC, SCC, and melanocytic lesions by linear discriminant analyses was 93.5% accurate.[64]

Complete absorption of mid-IR light results with samples greater than 10 to 15 mm in thickness, when in contrast, near-IR light is scattered to a much greater extent than it is absorbed, making tissues relatively transparent to near-IR light, thus allowing the examination of much larger volumes of *in vivo* tissue.[66] *In vivo* near-IR spectroscopic characterization of skin tumors presented by McIntosh et al., [67] for differential diagnosis of BCC from other skin cancer types, where linear discriminant analysis (LDA) was used to determine whether spectra could be classified according to lesion type. This resulted in accuracy of 70% to 98% in differentiating benign from premalignant or malignant lesions.

In 2006, Salomatina et al.[49] determined and compared the *in vitro* NIR spectroscopic properties of human skin to those of NMSC. They observed a significant difference in the NIR scattering between cancerous tissues and control skin, and noted that the absorption was significantly lower for BCC than for control skin.

A combination of infrared spectroscopy with high pressure (pressure-tuning infrared spectroscopy) was reported by Wong et al.[68] who worked with cluster analysis in 1992 and applied it to the study of paired sections of BCC and normal skin from 10 patients. Atmospheric pressure IR spectra of BCC were dramatically different from those of the corresponding normal skin. Compared to their normal controls, BCCs displayed increased hydrogen bonding of the phosphodiester group of nucleic acids, decreased hydrogen bonding of the C-OH groups of proteins, increased intensity of the band at 972 cm^{-1}, decreased intensity ratio between the CH_3 stretching and CH_2 stretching bands and accumulation of unidentified carbohydrates.

6 Laser-Scanning Microscopy

Within the last years, laser spectroscopic methods have achieved substantial improvements in the imaging of dermal tissue *in vivo*. With the recent development of *in vivo* LSM systems, which can be directly applied on any human skin area, new promising potentials have opened up for LSM in medicine. Laser-scanning microscopy allows the distinction of all types and formations of cells, as well as skin appendages, such as sweat glands and hair follicles. The laser-scanning microscopes are fiber-based systems which allow the investigation of all body sites. They have proved a potentially valuable diagnostic aid in BCC and SCC diagnosis, both *ex vivo* and *in vivo*.[69,70]

The basic confocal-principle involves focusing a laser light onto a small spot within the dermal tissue. A light signal out of the focus point is collected at the same time in order to create a confocal image. Mainly the returning light directly from the focal point is only detected, whilst prevention of any scattered and reflected light from out-of-focus planes increases the imaging contrast. A deep scan can be performed easily by moving the light focus deeper into the tissue. As a result, different cell layers can be observed, the skin architecture can be studied without taking a destructive biopsy.[71]

There are three types of confocal spectroscopic methods in use: the reflectance, fluorescence, and the Raman spectroscopy.[72–74] Depending on the laser source like an Argon laser 488 nm, or a NIR diode laser at 830 nm, the detection system and the usage or not of a contrast dye, different dermatologic *in vivo* laser-scanning microscopes are now commercially available. In the case of reflectance confocal microscopy (RCM), systems illumination and detection takes place at the same wavelength. *in vivo* laser-scanning microscopy in reflectance and fluorescence mode generate horizontal optical sections at a resolution that is comparable to routine histology, but at the present time, these techniques are limited by their penetration depth.[4] Compared to routine histology, those images are oriented horizontally to skin surface (en face) and they are analyzed in gray scale. There are several advantages of *in vivo* laser-scanning microscopy (LSM) over conventional histology. The imaging is painless and noninvasive, causing no tissue damage or alteration by processing or staining. Another aspect is the rapidity with which the data can be collected, and the ability of LSM for repeated evaluations of dynamic processes in real time.

6.1 *Reflectance Confocal Microscopy*

Confocal scanning laser microscopy in the reflectance mode (RCM) is a recently developed noninvasive technique of skin imaging that has been shown to be useful in discriminating NMSC from normal skin, while it is said that has similar resolution like to that of conventional histopathology.[75,76] RCM is a dynamic examination, and it is possible to move the focus area within the three dimensions, which has been considered as an equivalent of serial sectioning in conventional histopathology.[77,78]

RCM permits the acquisition of dynamic images of the epidermis and papillary dermis with resolution at a cellular level.[79,80] Current CM systems have an axial resolution of 1 to 5 μm and a lateral resolution of 0.5 to 1 μm. Their main technical limitation is related to the penetration depth of imaging, which cannot be deeper than 200 to 300 μm.[79,80] Some confocal microscopy systems are based on reflectance measurements of structures with different refractive indices, where the visualization of skin structures (melanin, hemoglobin, etc.) is based on differences in different reflectivity. Generally, the higher the differences in the refractive index of skin structures, the stronger the contrast of the images. In particular, melanin and keratin have high refractive indices, producing a bright contrast in the LCM. Since these differences are minor in the human skin, high-contrast images can be obtained only by considerable technical effort.

In 2001, Selkin et al.[69] studied 115 BCC patients with *in vivo* RCM reported characteristics features and proposed a diagnostic algorithm. Multivariate analysis found 8 independent features distinguishing between BCC and other lesions examined (melanoma, nevi, SCC, actinic keratosis, solar lentigines). Positive features included: polarized in the honeycomb, linear telangiectasia-like horizontal vessels, basaloid cord or nodule, and epidermal shadow; while negative features included: nonvisible papillare, cerebriform nests, and disarrangement of the epidermal layer. In SCC, features were found irregular epithelial mass with a variable proportion of normal and atypical keratinocytes, along with areas of anaplasia.[69]

Rajadhyaksha et al.[81] have used thick skin excisions to potentially guide Mohs micrographic surgery without frozen histopathology. Precise removal of nonmelanoma cancers with

minimum damage to the surrounding normal skin was guided by the histopathologic examination of each excision during Mohs micrographic surgery where real-time confocal reflectance microscopy offered an imaging method potentially to avoid frozen histopathology and prepare noninvasive (optical) sections within 5 min. However, they suggested that infrared RCM using acetic acid as a contrast agent was not a reliable method for the diagnosis of infiltrative BCC, mainly due to the intrinsically high scattering of dermal collagen that is around the thin strands of cancerous cells of this type of BCC.[81]

In another study of Gerger et al.[82] which included 20 patients with histologically verified BCC, an evaluation of fresh BCC excisions by confocal laser-scanning microscopy was performed by 4 independent observers. Logistic regression analysis revealed that mainly tumor cell nuclei and tumor nests should be taken into account for diagnostic decisions, whereas disintegration of tumor cells, peripheral palisading, and retraction of stroma were rarely useful. However, most of the features were highly reliable. The authors stated that this diagnostic validation study of RCM in microscopy-guided surgery yielded promising results in the microsurgery of any skin cancer. The same group[83] investigated the use of RCM in microsurgery for invasive SCCs and the results regarding the sensitivity and specificity of the method were very good and promising.

In vivo RCM has been used by Guitera et al.[84] for the evaluation of 710 consecutive cutaneous lesions excised to exclude malignancy. The authors proposed a two-step method of early diagnosing BCC and then melanoma, with 100% sensitivity and 88.5% specificity for BCC diagnosis.

6.2 *Fluorescence Confocal Laser-Scanning Microscope*

Fluorescence confocal laser-scanning microscopy (FLSM) *in vivo* is a novel technique where fluorophore distribution in the skin may illustrate morphologic changes in the epidermis. FLSM images have a high resolution of about 0.5 to 1 μm. The underlying principle of FLSM systems is the excitation and detection of fluorophores by scanning a focal plane within the tissue using a coherent laser light source. After excitation, the emitted fluorescence from the accumulation of exogenously applied fluorophores allows visualization of the intercellular and intracellular compartments of live skin.[4] An application for FLSM is the ability to image fluorescent markers that target specific subcellular molecules including proteins and therefore through the representation of cellular microscopy, to monitor specific pathologic and immune processes over time.[85]

FLSM study by Astner et al.,[4] using an argon-ion laser (488 nm) as the excitation light source, evaluated noninvasively NMSC *in vivo*, after intraepidermal injection of 0.2% sodium fluorescein (15 patients with BCC versus 10 healthy controls). FLSM was able to detect the morphologic characteristics of BCC that were in correlation with routine H&E histology. Tumor nests corresponded to the presence of islands of atypical basal cells that were monomorphic in shape. Large, elongated nuclei were often oriented along the same axis, resulting in an overall polarized appearance. Areas of clefting demarcated the tumor nests against surrounding epidermal structures. A superficial inflammatory infiltrate was visualized. Epidermal pleomorphism, the characteristic nesting of atypical basal cells, and increased blood vessel tortuosity was visualized.[4]

6.2.1 *Multiphoton tomography*

MPT can exploit autofluorescence of intrinsic tissue fluorophores (NADH, cholecalciferol, flavins, keratins, elastin, collagen), thereby enabling functional and structural imaging of the skin. In conventional confocal fluorescence microscopy, fluorophores are excited in the visible or UV spectrum, while MPT excitation involves the simultaneous absorption of two or more photons of longer wavelength, usually in the near-infrared spectrum. This longer wavelength infrared radiation undergoes less scattering than visible light, thus facilitating high resolution imaging deeper into biological tissue. Efficient MPT excitation usually requires ultrashort femtosecond laser pulses, which are also able to produce the nonlinear effect of second harmonic generation (SHG), engendered by periodic structures in tissue matrix components such as collagen. The combination of autofluorescence imaging and SHG gives access to morphology and structure of both cells and extracellular matrix of the skin.[86]

Multiphoton laser tomography (MPT) has been combined with fluorescence lifetime imaging (FLIM). FLIM is an additional noninvasive microscopy technique enabling the identification of endogenous fluorescent molecules and their surrounding medium by measuring the decay rate of fluorescence emission. A commercially available MPT imaging system consisting of three major modules: excitation laser (titanium–sapphire laser), scanning unit, and control module, has been used to provide BCC descriptors and to successfully diagnose 63 BCC *ex vivo*.[86] Furthermore, results obtained with MPT-FLIP imaging are comparable with those obtained with RCM.[87]

6.3 *Confocal Raman Laser-Scanning Microscope*

CLSM is based on the detection of Raman spectra in the focal plane. Raman scattering is caused by tissue molecules or topically applied substances, where molecular bonds demonstrate specific spectral signatures. Compared to fluorescence and reflection LSM, Raman microscopy does not deliver an image of the morphological structure but it rather provides chemical information with regard to the tissue. There is low experience in diagnosis of NMSC with CLSM. However, clinical application has been investigated in studies of BCC.[58,88,89] Research and full development in the clinical field is under investigation.

6.4 *Combination of Fluorescence, Reflectance, and Raman Mode on Laser-Scanning Microscopy*

Combinations of fluorescence and Raman spectroscopic laser-scanning measurements can be used in skin physiology, pharmacology for the analysis of the distribution and the penetration process of topically applied substances, or for the increase of contrast and differentiated correlation.[90,91,92]

Dye-enhanced [methylene blue (MB), toluidine blue (TB), belonging to the family of phenothiazinium dyes] multimodal, reflectance, fluorescence, and fluorescence polarization confocal microscopy was studied by Al-Arash et al.[90] in fresh thick human NMSC with 37 samples for the reliable *in vitro* detection of BCC and SCC. Reflectance, fluorescence, and fluorescence polarization of TB and MB were excited using 633 and 656 nm laser light, respectively, and reflectance images at 830 nm were used as a reference. Compared to H&E histopathology, similar results were reported for reflectance and fluorescence confocal mosaics.

Skvara et al.[91] studied the fluorescence properties of the fluorophore indocyanine green (ICG) and reflectance versus fluorescence images after its application to human skin. Intradermal application of a 0.5% solution of ICG was intradermally injected in 3 patients with BCC. The tissue was illuminated with near-infrared laser light (785 nm) and reflectance and fluorescence images were obtained using a commercially available confocal laser-scanning microscope. Typical tumor nests were identified, characterized by polarization of epithelial cells at the periphery of the islands. The two confocal modes showed different accuracy in recognizing these tumor islands, with better precision in FLSM than in RCM.

7 Optical Coherence Tomography

Optical coherence tomography (OCT), another type of optical imaging modality, was first demonstrated in 1991.[93] In particular, OCT, an interferometry-based method, performs high resolution, cross-sectional tomographic imaging of the internal microstructure of skin by measuring backscattered and back reflected light and has been recognized as a promising tool for the diagnosis of pathological changes.[94] OCT has greater image resolution than ultrasound, typically 5 to 15 μm. Compared to confocal microscopy and multiphoton microscopy, OCT has a larger field of view and penetration depth and offers cross-sectional images of the skin similar to histopathology sections.[95]

However, in a highly scattering tissue like skin, OCT has a relatively limited penetration depth of up to 2 mm, since this method operates with ballistic photons,[5,96,97] while lateral resolution of 10 to 15 μm is more typical.[94,95,97–101] New systems with ultra-high resolution of about 1 μm have recently been developed. OCT uses wavelengths within the band 600 to 2000 nm where the main constituents of the tissue, water, pigments, etc. exhibit low absorption.[5] In order to obtain maximum penetration depth, matching index gel can be applied in the skin tissue or we could use longer wavelengths around 1300 nm, while for a better image contrast, central wavelengths around 800 nm are more appropriate.[102] Broadband sources such as superluminescent diodes, semiconductor-based light sources, or femtosecond lasers (e.g., $Ti:Al_2O_3$) have short coherence lengths and thus are good candidates for use in OCT.[103]

Some OCT scanners for dermatological purposes are already available on a commercial basis.[104] OCT can reliably identify epidermis and the dermo-epidermal junction (DEJ),[105] while it is also able to identify the normal regional differences.[105] It has shown promise as a diagnostic tool for the detection and imaging of NMSC.[5,94,100] A breakup of the characteristic layering of normal skin[105,106] is found in OCT images of NMSC lesions.[5,94,100,106–108] However, this disruption of layering is also seen in various benign lesions as sebhorreic keratosis[108] and benign melanocytic nevi.[109] Gambichler et al.[94] confirmed with their experiments that thinning of the epidermal layer corresponded to severe actinic changes including epidermal atrophy, as shown in histology. Moreover, faint lobular structures, often appearing in honeycomb-like aggregates, could be visualized in the upper dermis. These structures usually had a signal-poor core surrounded by a light backscattering ring.[94]

Gambichler et al.,[104] in a more systematic study, found a loss of normal skin architecture and a disarrangement of the epidermis and upper dermis on OCT images of BCCs as compared with adjacent nonlesional skin. Furthermore, large plug-like signal-intense structures, honeycomb-like signal-free structures, and prominent signal-free cavities in the upper dermis were requently detected.

Several other NMSC features in OCT images have been described. The most important are: focal changes including thickening of epidermis (AK);[5,110] dark rounded areas, sometimes surrounded by a white area (BCC basaloid island cell clusters and surrounding stroma); and increased penetration depth in OCT images.[5,94]

Mongensen et al.[97,111] found a sensitivity of 79% to 94% and specificity of 85% to 96% in differentiating normal skin from lesions for OCT. Discrimination of AK from BCC was not possible in their research.

Other studies also suggested a good match between OCT images and histopathology in BCC lesions,[107] although BCC subtypes could not be identified in OCT images.[112] In the previous year, Olmedo et al.[107] performed an interesting OCT study on BCC where they found lobules, islands, and infiltrating strands of BCC appeared similar in OCT images and histologic sections regardless of the type of BCC. Notably, Olmedo et al.[107] reported that multifocal superficial BCC can be differentiated from other BCC subtypes. In addition, the tumor tissue observed in the deeper dermis appeared as signal-poor round structures due to penetration depth of OCT. In that matter, when Korde et al.[110] examined superficial BCC, a subepidermal highly reflecting band was found in the OCT image that corresponded to the tumor in histological sections.

SCC has mainly been studied on oral mucosal surfaces using OCT, but changes similar to BCC have been described.[113] Coleman et al.[114] confirmed previous reports of the limitation in the use of OCT in SCC,[97,101,110] where there is shadowing by surface hyperkeratosis.

An advanced version of OCT, the polarization-sensitive OCT (PS-OCT) has the ability to visualize and quantify the birefringence properties of skin and thus has been used as an efficient tool for tissue segmentation.[104] Many types of tissue are distinguishable in PS-OCT, in particular those with a significant collagen content such as the skin.[104,105] Several types of invasive lesions, including BCC, can cause a breakdown of collagen structure, resulting in a loss of birefringence which has been quantified using PS-OCT.[100,115]

In most researchers work, no statistically significant difference was found with conventional OCT between nodular, multifocal superficial, and infiltrative BCC. This may be due to the relatively small sample size in studies of BCC subtypes such as multifocal superficial BCC and infiltrative BCC.[94] In this matter, nowadays a newer developed version of OCT with high-definition facilitates *in vivo* diagnosis of BCC and allows the distinction between different BCC subtypes for increased clinical utility.[115]

This is an innovative technique based on the principle of conventional OCT, with the ability to carry out optical imaging up to 570 μm deep within highly scattering media such as skin and with a μm resolution in both lateral and axial directions, giving it the potential to visualize individual cells.[115] Instead of a single pin diode, it uses a two-dimensional, infrared-sensitive (1000 to 1700 nm) imaging array for light detection. This enables focus tracking: the focal plane is continuously moved through the sample,[116] which in addition to the vertical OCT imaging mode offers a real-time, horizontal, so-called en-face imaging mode, which allows the immediate visualization of OCT pictures with high resolution in both dimensions.[117]

On the other hand, the higher resolution results in a reduced penetration depth making HD-OCT not the medium of choice for the measurement of thick tumors. Here, conventional OCT with a reported penetration depth of nearly 1 to 2 mm seems to be superior.[117] Nevertheless, HD-OCT may serve as an important adjunct which may reduce the need for invasive biopsies in some of the cases, e.g., multiple tumor or patients who may request nonsurgical therapy. In such cases, HD-OCT makes it possible to conduct longitudinal studies of lesional therapy such as PDT or other nonsurgical treatment procedures.[116]

It may be advantageous to combine OCT with other imaging modalities, in the so called multimodality imaging such as Raman, Doppler, fluorescence, and ultrasound. This approach may further improve diagnostic capabilities in skin research as well as future dermatology practice.

8 Conclusions

Novel and established diagnostic techniques, involving spectroscopic and imaging diagnosis for NMSC have been reviewed in this article. Some of these novel techniques have the potential to become clinically available for the noninvasive diagnosis of NMSC. Many of these diagnostic methods seem to offer an adequate diagnostic accuracy, especially as a supplement to clinical diagnosis. The optical imaging technologies, such as fluorescence diffuse reflectance, Raman and near-infrared spectroscopy, optical coherence tomography, and confocal laser-scanning microscopy have been discussed for their resolution and accuracy in dermatological diagnosis. While the skin biopsy and histopathological assessment are yet to be replaced, the evolution and combination of spectroscopic techniques may be a promising technology for the photodiagnosis of NMSC, in the future.

Acknowledgments

We would like to gratefully acknowledge Dr. A. A. Serafetinides and Dr. M. Makropoulou, professors of the Physics Department, School of Applied Mathematical and Physical Sciences, National Technical University of Athens, Greece for providing access to their facility and for their assistance with the spectroscopic measurements. We also thank A Tsenga for her help in the histopathology examination of the samples.

References

1. E. Drakaki et al., "Laser-induced fluorescence and reflectance spectroscopy for the discrimination of basal cell carcinoma from the surrounding normal skin tissue," *Skin Pharmacol. Physiol.* **22**(3), 158–165 (2009).
2. C. Dessinioti et al., "Basal cell carcinoma: what's new under the sun," *Photochem. Photobiol.* **86**(3), 481–491 (2010).
3. C. Dessinioti, C. Antoniou, and A. J. Stratigos, "New targeted approaches for the treatment and prevention of nonmelanoma skin cancer," *Exp. Rev. Dermatol.* **6**(6), 625–634 (2011).
4. S. Astner et al., "Clinical applicability of in vivo fluorescence confocal microscopy for noninvasive diagnosis and therapeutic monitoring of nonmelanoma skin cancer," *J. Biomed. Opt.* **13**(1), 014003 (2008).
5. M. Mogensen and G. B. E. Jemec, "Accuracy in the diagnosis of nonmelanoma skin cancer, non-surgical treatment of keratinocyte skin cancer," Chapter 6, in *Non-Surgical Treatment of Keratinocyte Skin Cancer*, G. B. E. Jemec, L. Kemeny, and D. Miech, Eds., Springer, Berlin (2009).
6. G. A. Wagnieres, W. M. Star, and B. C. Wilson, "*In vivo* fluorescence spectroscopy and imaging for oncological applications," *Photochem. Photobiol.* **68**(5), 603–663 (1998).
7. I. Georgakoudi et al., "Fluorescence, reflectance, and light-scattering spectroscopy for evaluating dysplasia in patient with Barrett's esophagus," *Gastroenterology* **120**(7), 1620–1629 (2001).
8. I. Georgakoudi et al., "Trimodal spectroscopy for the detection and characterization of cervical precancers *in vivo*," *Am. J. Obstet. Gynecol.* **186**(3), 374–382 (2002).
9. F. Koenig et al., "Autofluorescence guided biopsy for the early diagnosis of bladder carcinoma," *J. Urol.* **159**(6), 1871–1875 (1998).
10. N. Kollias et al., "Endogenous skin fluorescence includes bands that may serve as quantitative markers of aging and photoaging," *J. Invest. Dermatol.* **111**(5), 776–780 (1998).
11. E. Drakaki, M. Makropoulou, and A. A. Serafetnindes, "*In vitro* fluorescence measurements and Monte Carlo simulation of laser irradiation propagation in porcine skin tissue," *Lasers Med. Sci.* **23**(3), 267–76 (2008).
12. N. Kollias, G. Zonios, and G. Stamatas, "Fluorescence spectroscopy of skin," *Vibrat. Spectrosc.* **28**(1), 17–24 (2002).
13. J. Bigio and J. R. Mourant, "Ultraviolet and visible spectroscopies for tissue diagnostics: fluorescence spectroscopy and elastic-scattering spectroscopy," *Phys. Med. Biol.* **42**(5), 803–814 (1997).
14. E. Borisova et al., "Qualitative optical evaluation of malignancies related to cutaneous phototype," *Proc. SPIE* **7563**, 75630X (2010).
15. Q. Liu, "Role of optical spectroscopy using endogenous contrasts in clinical cancer diagnosis," *World J. Clin. Oncol.* **2**(1), 50–63 (2011).
16. R. Na, I. M. Stender, and H. C. Wulf, "Can autofluorescence demarcate basal cell carcinoma from normal skin? a comparison with protoporphyrin IX fluorescence," *Acta Derm. Venereol.* **81**(4), 246–249 (2001).
17. A. Pena et al., "Spectroscopic analysis of keratin endogenous signal for skin multiphoton microscopy," *Opt. Express* **13**(16), 6268–6274 (2005).
18. N. Ramanujam, "Fluorescence spectroscopy of neoplastic and non-neoplastic tissues," *Neoplasia* **2**(1–2), 89–117 (2000).
19. E. Borisova et al., "Optical biopsy of human skin—a tool for cutaneous tumours' diagnosis," *Int. J. Bioautomat.* **16**(1), 53–72 (2012).
20. L. Brancaleon et al., "*In vivo* fluorescence spectroscopy of nonmelanoma skin cancer," *Photochem. Photobiol.* **73**(2), 178–183 (2001).
21. H. Zeng et al., "Autofluorescence properties of skin and applications in dermatology," *Proc SPIE* **4224**, 366–373 (2000).
22. M. Panjehpour et al., "Laser-induced fluorescence spectroscopy for *in vivo* diagnosis of non-melanoma skin cancers," *Lasers Surg. Med.* **31**(5), 367–373 (2002).
23. T. Vo-Dinh et al., "Laser-induced fluorescence for the detection of esophageal and skin cancer," *Proc SPIE* **4958**, 67–70 (2003).
24. H. Zeng et al., "Autofluorescenceof basal cell carcinoma," *Proc. SPIE* **3245**, 314–317 (1998).
25. E. Borisova et al., "Light-induced fluorescence spectroscopy and optical coherence tomography of basal cell carcinoma," *J. Innov. Opt. Health Sci.* **2**(3), 261–268 (2009).
26. E. Borisova, P. Troyanova, and L. Avramov, "Optical biopsy of non-melanin pigmented cutaneous benign and malignant lesions," *Proc. SPIE* **6257**, 62570U (2006).
27. R. Richards-Kortum and E. Sevick-Muraca, "Quantitative optical spectroscopy for tissue diagnostics," *Annu. Rev. Phys. Chem.* **47**, 555–606 (1996).
28. N. Rajaram et al., "Pilot clinical study for quantitative spectral diagnosis of non-melanoma skin cancer," *Lasers Surg. Med.* **42**(10), 716–727 (2010).
29. P. G. Lang and J. C. Maize, "Basal cell carcinoma," in *Cancer of the Skin*, D. S. Rigel et al., Eds., pp. 101–132, Elsevier Saunders, Philadelphia, PA, (2005).
30. M. E. Nolen et al., "Nonmelanoma skin cancer: part 1," *J. Dermatol. Nurses' Assoc.* **3**(5), 260–281 (2011).
31. L. R. Braathen et al., "Guidelines on the use of photodynamic therapy for nonmelanoma skin cancer: an international consensus," *J. Am. Acad. Dermatol.* **56**(1), 125–143 (2007).
32. M. M. Kleinpenning, "Diagnostic and therapeutic innovations of phototherapy in psoriasis and (pre)malignancies of the skin," PhD Thesis, Radboud University Nijmegen Medical Centre, Nijmegen, The Netherlands (2010).
33. N. Van der Beek et al., "PpIX fluorescence combined with autofluorescence is more accurate than PpIX fluorescence alone in fluo-

rescence detection of non-melanoma skin cancer: an intra-patient direct comparison study," *Lasers Cutan. Surg.* **44**(4), 271–276 (2012).
34. J. de Leeuw et al., "Fluorescence detection and diagnosis of non-melanoma skin cancer at an early stage," *Lasers Surg. Med.* **41**(2), 96–103 (2009).
35. M. B. Ericson et al., "Bispectral fluorescence imaging combined with texture analysis and linear discrimination for correlation with histopathologic extent of basal cell carcinoma," *J. Biomed. Opt.* **10**(3), 034009 (2005).
36. C. Sandberg et al., "Fluorescence diagnostics of basal cell carcinomas comparing methyl-aminolaevulinate and aminolaevulinic acid with visual clinical tumour size," *Acta. Derm. Venereol.* **91**(4), 398–403 (2011).
37. C. Fritsch et al. "Preferential relative porphyrin enrichment in solar keratoses upon topical application of delta-aminolevulinic acid methylester," *Photochem. Photobiol.* **68**(2), 218–221 (1998).
38. J. Moan, L. W. Ma, and V. Iani, "On the pharmacokinetics of topically applied 5-aminolevulinic acid and two of its esters," *Int. J. Cancer* **92** (1), 139–143 (2001).
39. M. M. Kleinpenning et al., "Fluorescence diagnosis in actinic keratosis and squamous cell carcinoma," *Photodermatol. Photoimmunol. Photomed.* **26**(6), 297–302 (2010).
40. E. Tierney, J. Petersen, and W. Hanke, "Photodynamic diagnosis of tumor margins using methyl aminolevulinate before Mohs micrographic surgery," *J. Am. Acad. Dermatol.* **64**(5), 911–918 (2011).
41. T. Wetzig et al., "No clinical benefit of preoperative fluorescence diagnosis of basal cell carcinoma localized in the H-zone of the face," *Br. J. Dermatol.* **162**(6), 1370–1376 (2010).
42. X. Zhang et al., "Fluorescence examination and photodynamic therapy of facial squamous cell carcinoma—a case report," *Photodiagnosis Photodyn. Ther.* **9**(1), 87–90 (2012).
43. C. Y. Lee, K. H. Kim, and Y. H. Kim, "The efficacy of photodynamic diagnosis in defining the lateral border between a tumor and a tumor-free area during Mohs micrographic surgery," *Dermatol. Surg.* **36**(11), 1704–1710 (2010).
44. A. N. Yaroslavsky et al., "Fluorescence polarization of tetracycline as a technique for mapping nonmelanoma skin cancer," *J. Biomed. Opt.* **12**(1), 014005 (2007).
45. A. Garcia-Uribe et al., "Skin cancer detection by spectroscopic oblique-incidence reflectometry: classification and physiological origins," *Appl. Opt.* **43**(13), 2643–2650 (2004).
46. M. Mehrübeoğlu et al., "Skin lesion classification using oblique-incidence diffuse reflectance spectroscopic imaging," *Appl. Opt.* **41**(1), 182–192 (2002).
47. R. Marchesini et al., "In vivo spectrophotometric evaluation of neoplastic and non-neoplastic skin pigmented lesions—I. Reflectance measurements," *Photochem. Photobiol.* **53**(1), 77–84 (1991).
48. A. J. Thompson et al., "*In vivo* measurements of diffuse reflectance and time-resolved autofluorescence emission spectra of basal cell carcinomas," *J. Biophoton.* **5**(3), 240–254 (2012).
49. E. Salomatina et al., "Optical properties of normal and cancerous human skin in the visible and near-infrared spectral range," *J. Biomed. Opt.* **11**(6), 064026 (2006).
50. N. Rajaram et al., "Experimental validation of the effects of microvasculature pigment packaging on *in vivo* diffuse reflectance spectroscopy," *Lasers Surg. Med.* **42**(7), 680–688 (2010).
51. S. Fendel and B. Schrader, "Investigation of skin lesions by NIR-FT-Raman spectroscopy," *Fresenius J. Anal. Chem.* **360**(5), 609–613 (1998).
52. M. Gniadecka et al., "Melanoma diagnosis by Raman spectroscopy and neural network: structure alterations in proteins and lipids in intact cancer tissue," *J. Invest. Dermatol.* **122**(2), 443–449 (2004).
53. L. D. Nunes et al., "FT-Raman spectroscopy study for skin cancer diagnosis," *Spectrosc. Int. J.* **17**(2–3), 597–602 (2003).
54. B. Schrader et al., "NIR FT Raman spectroscopy-a new tool in medical diagnostics," *J. Mol. Struct.* **408/409**, 23–31 (1997).
55. N. Skrebova, Y. Ozaki, and S. Arase, "Noninvasive quantification of cutaneous oedema in patch test reactions by fiber optic near-infrared fourier transform Raman spectroscopy," *Subsurf. Sens. Technol. Appl.* **3**(1), 19–34 (2002).
56. B. W. Barry, H. G. M. Edwards, and A. C. Williams, "Fourier transform Raman and infrared vibrational study of human skin: assignment of spectral bands," *J. Raman Spectrosc.* **23**(11), 641–645 (1992).
57. M. Gniadecka et al., "Diagnosis of basal cell carcinoma by Raman spectroscopy," *J. Raman Spectrosc.* **28**(2–3), 125–129 (1997).
58. A. Nijssen et al., "Discriminating basal cell carcinoma from its surrounding tissue by Raman spectroscopy," *J. Invest. Dermatol.* **119**(1), 64–69 (2002).
59. L. Silveira, Jr. et al., "Diagnosing basal cell carcinoma in vivo by near-infrared Raman spectroscopy: a principal components analysis discrimination algorithm," *Proc. SPIE* **8207**, 82070X (2012).
60. R. de M. F. Pereira et al., "Diagnosis of squamous cell carcinoma of human skin by Raman spectroscopy," *Proc. SPIE* **5326**, 106–112 (2004).
61. J. Choi et al., "Direct observation of spectral differences between normal and basal cell carcinoma (BCC) tissues using confocal Raman microscopy," *Biopolymers* **77**(5), 264–272 (2005).
62. C. A. Lieber et al., "In vivo nonmelanoma skin cancer diagnosis using Raman microspectroscopy," *Lasers Surg. Med.* **40**(7), 461–467 (2008).
63. K. Cal, J. Stefanowska, and D. Zakowiecki, "Current tools for skin imaging and analysis," *Int. J. Dermatol.* **48**(12), 1283–1289 (2009).
64. L. M. McIntosh et al., "Infrared spectra of basal cell carcinomas are distinct from non-tumor-bearing skin components," *J. Invest. Dermatol.* **112**(6), 951–956 (1999).
65. L. M. McIntosh et al., "Analysis and interpretation of infrared microscopic maps: visualisation and classifcation of skin components by digital staining and multivariate analysis," *Biospectroscopy* **5**(5), 265–275 (1999).
66. M. Laura et al., "Towards non-invasive screening of skin lesions by near- infrared spectroscopy," *J. Invest. Dermatol.* **116**(1), 175–181 (2001).
67. L. M. McIntosh et al., "Near-infrared spectroscopy for dermatological applications," *Vib. Spectrosc.* **28**(1), 53–58 (2002).
68. P. T. T. Wong et al., "Distinct infrared spectroscopic patterns of human basal cell carcinoma of the skin," *Cancer Res.* **53**(4), 762–765 (1993).
69. B. Selkin et al., "*In vivo* confocal microscopy in dermatology," *Dermatol. Clin.* **19**(2), 369–377 (2001).
70. V. Q. Chung et al., "Use of *ex vivo* confocal scanning laser microscopy during Mohs surgery for nonmelanoma skin cancers," *Dermatol. Surg.* **30**(12 Pt 1), 1470–1478 (2004).
71. L. E. Meyer and J. Lademann, "Application of laser spectroscopic methods for in vivo diagnostics in dermatology," *Laser Phys. Lett.* **4**(10), 754–760 (2007).
72. D. Rallan and C. C. Harland, "Skin imaging: is it clinically useful?," *Clin. Exp. Dermatol.* **29**(5), 453–459 (2004).
73. N. Aspres et al., "Imaging the skin," *Austral. J. Dermatol.* **44**(1), 19–27 (2003).
74. M. Ulrich et al., "Noninvasive diagnostic tools for nonmelanoma skin cancer," *Br. J. Dermatol.* **157**(suppl 2), 56–85 (2007).
75. M. Rajadhyaksha et al., "*In vivo* confocal scanning laser microscopy of human skin II: advances in instrumentation and comparison with histology," *J. Invest. Dermatol.* **113**(3), 293–303 (1999).
76. M. Mogensen and G. B. Jemec, "Diagnosis of nonmelanoma skin cancer/keratinocyte carcinoma: a review of diagnostic accuracy of nonmelanoma skin cancer diagnostic tests and technologies," *Dermatol. Surg.* **33**(10), 1158–1174 (2007).
77. S. Debarbieux et al., "Perioperative confocal microscopy of the nail matrix in the management of in situ or minimally invasive subungual melanomas," *Br. J. Dermatol.* **167**(4), 828–836 (2012).
78. S. Gonzalez and Z. Tannous, "Real-time, *in vivo* confocal reflectance microscopy of basal cell carcinoma," *J. Am. Acad. Dermatol.* **47**(6), 869–874 (2002).
79. P. Calzavara-Pinton et al., "Reflectance confocal microscopy for *in vivo* skin imaging," *Photochem. Photobiol.* **84**(6), 1421–1430 (2008).
80. D. S. Gareau, Y. G. Patel, and M. Rajadhyaksha, "Basic principles of reflectance confocal microscopy," in *Reflectance Confocal Microscopy of Cutaneous Tumors*, S. Gonzalez, M. Gill, and A. C. Halpern, Eds., pp. 1–13, Informa, London (2008).
81. M. Rajadhyaksha et al., "Confocal examination of nonmelanoma cancers in thick skin excisions to potentially guide mohs micrographic

surgery without frozen histopathology," *J. Invest. Dermatol.* **117**(5), 1137–1143 (2001).
82. A. Gerger et al., "Confocal examination of untreated fresh specimens from basal cell carcinoma: implications for microscopically guided surgery," *Arch. Dermatol.* **141**(10), 1269–1274 (2005).
83. M. Horn et al., "The use of confocal laser-scanning microscopy in microsurgery for invasive squamous cell carcinoma," *Br. J. Dermatol.* **156**(1), 81–84 (2007).
84. P. Guitera et al. "In vivo confocal microscopy for diagnosis of melanoma and basal cell carcinoma using a two-step method: analysis of 710 consecutive clinically equivocal cases," *J. Invest. Dermatol.* **132**(10), 2386–2394 (2012).
85. C. Suihko et al., "Fluorescence fibreoptic confocal microscopy of skin *in vivo*: microscope and fluorophores," *Skin Res. Technol.* **11**(4), 254–267 (2005).
86. S. Seidenari et al., "Multiphoton laser tomography and fluorescence lifetime imaging of basal cell carcinoma: morphologic features for non-invasive diagnostics," *Exp. Dermatol.* 21(11), 831–836 (2012).
87. M. Manfredini et al., "High-resolution imaging of basal cell carcinoma: a comparison between multiphoton microscopy with fluorescence lifetime imaging and reflectance confocal microscopy," *Skin Res. Technol.* [Epub ahead of print] (2012).
88. K. U. Schallreuter et al., "*In vivo* and *in vitro* evidence for hydrogen peroxide (H2O2) accumulation in the epidermis of patients with vitiligo and its successful removal by a UVB-activated pseudocatalase," *J. Invest. Dermatol. Symp. Proc.* **4**(1), 91–96 (1999).
89. J. Wohlrab et al., "Noninvasive characterization of human stratum corneum of undiseased skin of patients with atopic dermatitis and psoriasis as studied by Fourier transform Raman spectroscopy," *Biopolym.* **62**(3), 141–146 (2001).
90. M. Y. Al-Arashi, E. Salomatina, and A. N. Yaroslavsky, "Multimodal confocal microscopy for diagnosing nonmelanoma skin cancers," *Lasers Surg. Med.* **39**(9), 696–705 (2007).
91. H. Skvara et al., "*In vivo* fluorescence confocal microscopy: indocyanine green enhances the contrast of epidermal and dermal structures," *J. Biomed. Opt.* **16**(9), 096010 (2011).
92. T. Vergou et al., "Comparison between TEWL and laser scanning microscopy measurements for the *in vivo* characterization of the human epidermal barrier," *J. Biophoton.* **5**(2), 152–158 (2012).
93. D. Huang et al., "Optical coherence tomography," *Science* **254**(5035), 1178–1181 (1991).
94. T. Gambichler et al., "*In vivo* optical coherence tomography of basal cell carcinoma," *J. Dermatol Sci.* **45**(3), 167–173 (2007).
95. J. K. Barton et al., "Investigating sun-damaged skin and actinic keratosis with optical coherence tomography: a pilot study," *Technol. Cancer Res. Treat.* **2**(6), 525–535 (2003).
96. A. Gh. Podoleanu, "Optical coherence tomography," *Br. J. Radiol.* **78**(935), 976–988 (2005).
97. M. Mogensen et al., "Optical coherence tomography for imaging of skin and skin diseases," *Semin. Cutan. Med. Surg.* **28**(3), 196–202 (2009).
98. J. G. Fujimoto et al., "Optical coherence tomography: an emerging technology for biomedical imaging and optical biopsy," *Neoplasia* **2**(1–2), 9–25 (2000).
99. M. Vogt et al., "Comparison of high frequency ultrasound and optical coherence tomography as modalities for high resolution and non invasive skin imaging," *Biomedizinische Technik/Biomed. Eng.* **48**(5), 116–121 (2003).
100. M. C. Pierce et al., "Advances in optical coherence tomography imaging for dermatology," *J. Invest. Dermatol.* **123**(3), 458–463 (2004).
101. T. Gambichler et al., "Applications of optical coherence tomography in dermatology," *J. Dermatol. Sci.* **40**(2), 85–94 (2005).
102. A. Alex et al., "Multispectral *in vivo* three-dimensional optical coherence tomography of human skin," *J. Biomed. Opt.* **15**(2), 026025 (2010).
103. J. G. Fujimoto, "Optical coherence tomography: introduction," in *The Handbook of Optical Coherence Tomography*, B. E. Bouma and J. G. Tearney, Eds., Marcel Dekker, Inc., New York, NY (2001).
104. T. Gambichler, V. Jaedicke, and S. Terras, "Optical coherence tomography in dermatology: technical and clinical aspects," *Arch. Dermatol. Res.* **303**(7), 457–473 (2011).
105. M. Mogensen et al., "Morphology and epidermal thickness of normal skin imaged by optical coherence tomography," *Dermatology* **217**(1), 14–20, (2008).
106. R. Steiner, R. K. Kunzi, and K. K. Scharffetter, "Optical coherence tomography: clinical applications in dermatology," *Med. Laser Appl.* **18**(3), 249–259 (2003).
107. J. M. Olmedo et al., "Optical coherence tomography for the characterization of basal cell carcinoma *in vivo*: a pilot study," *J. Am. Acad. Dermatol.* **55**(3), 408–12 (2006).
108. J. Welzel, "Optical coherence tomography in dermatology: a review," *Skin Res. Technol.* **7**(1), 1–9 (2001).
109. T. Gambichler et al., "Characterization of benign and malignant melanocytic skin lesions using optical coherence tomography *in vivo*," *J. Am. Acad. Dermatol.* **57**(4), 629–637 (2007).
110. V. R. Korde et al., "Using optical coherence tomography to evaluate skin sun damage and precancer," *Lasers Surg. Med.* **39**(9), 687–695 (2007).
111. M. Mogensen et al., "Assessment of OCT imaging in the diagnosis of non-melanoma skin cancer and benign lesions vs. normal skin: observer blinded evaluation by dermatologists and pathologists," *Dermatol. Surg.* **35**(6), 965–972 (2009).
112. L. K. Jensen et al., "Optical coherence tomography in clinical examination of non-pigmented skin malignancies," *Proc SPIE* **5140**, 160–167 (2003).
113. P. Wilder-Smith et al., "*In vivo* optical coherence tomography for the diagnosis of oral malignancy," *Lasers Surg. Med.* **35**(4), 269–275 (2004).
114. A. J. Coleman et al., "Histological correlates of optical coherence tomography in non-melanoma skin cancer," *Skin Res. Technol.* [Epub ahead of print] (2012).
115. J. Strasswimmer et al., "Polarization-sensitive optical coherence tomography of invasive basal cell carcinoma," *J. Biomed. Opt.* **9**(2), 292–298 (2004).
116. M. A. Boone et al., "Imaging of basal cell carcinoma by high-definition optical coherence tomography. Histomorphologic correlation a pilot study," *Br. J. Dermatol.* **167**(4), 856–864 (2012).
117. T. Maier et al., "Morphology of basal cell carcinoma in high definition optical coherence tomography: en-face and slice imaging mode, and comparison with histology," *J. Eur. Acad. Dermatol. Venereol.* [Epub ahead of print] (2012).